blood®
Regular Article

IMMUNOBIOLOGY AND IMMUNOTHERAPY

HSP-CAR30 with a high proportion of less-differentiated T cells promotes durable responses in refractory CD30$^+$ lymphoma

Ana Carolina Caballero,[1-3,*] Cristina Ujaldón-Miró,[1-3,*] Paula Pujol-Fernández,[1-3] Rosanna Montserrat-Torres,[1-3] Maria Guardiola-Perello,[1-3] Eva Escudero-López,[1-3] Irene Garcia-Cadenas,[1] Albert Esquirol,[1] Rodrigo Martino,[1] Paola Jara-Bustamante,[1-3] Pol Ezquerra,[4-6] José Manuel Soria,[4-6] Eva Iranzo,[1] Maria-Estela Moreno-Martinez,[6,7] Mireia Riba,[6,7] Jorge Sierra,[1,6] Carmen Alvarez-Fernández,[1-3,†] Laura Escribà-Garcia,[1-3,†] and Javier Briones[1-3,†]

[1]Hematology Service, Hospital de la Santa Creu i Sant Pau, Barcelona, Spain; [2]Laboratory of Experimental Hematology, Institut d'Investigació Biomèdica Sant Pau, Barcelona, Spain; [3]Josep Carreras Leukemia Research Institute, Barcelona, Spain; [4]Unit of Genomics of Complex Disease, Research Institute of Sant Pau Hospital, Barcelona, Spain; [5]Centre for Biomedical Network Research on Rare Diseases, Instituto de Salud Carlos III, Madrid, Spain; [6]Institut d'Investigació Biomèdica Sant Pau, Barcelona, Spain; and [7]Pharmacy Service, Hospital de la Santa Creu i Sant Pau, Barcelona, Spain

KEY POINTS

- CART30 with high proportion of less-differentiated memory T cells favors expansion and long-term persistence of memory CART30 cells.
- CART30 was used to treat 10 patients with refractory CD30$^+$ lymphoma, with 50% experiencing durable complete responses.

CD30-directed chimeric antigen receptor T-cell therapy (CART30) has limited efficacy in relapsed or refractory patients with CD30$^+$ lymphoma, with a low proportion of durable responses. We have developed an academic CART30 cell product (HSP-CAR30) by combining strategies to improve performance. HSP-CAR30 targets a proximal epitope within the nonsoluble part of CD30, and the manufacturing process includes a modulation of ex vivo T-cell activation, as well as the addition of interleukin-21 (IL-21) to IL-7 and IL-15 to promote stemness of T cells. We translated HSP-CAR30 to a phase 1 clinical trial of 10 patients with relapsed/refractory classic Hodgkin lymphoma (HL) or CD30$^+$ T-cell non-Hodgkin lymphoma. HSP-CAR30 was mainly composed of memory stem–like ($T_{SCM\text{-}like}$) and central memory (T_{CM}) CAR30$^+$ T cells (87.5% ± 5%). No dose-limiting toxicities were detected. Six patients had grade 1 cytokine release syndrome, and no patient developed neurotoxicity. The overall response rate was 100%, and 5 of 8 patients with HL achieved complete remission (CR). An additional patient with HL achieved CR after a second HSP-CAR30 infusion. Remarkably, 60% of patients have ongoing CR after a mean follow-up of 34 months. CAR30$^+$ T cells at expansion peak had a predominance of T_{SCM} and T_{CM} cells, and CAR30$^+$ T cells remained detectable in 3 of 5 evaluable patients at least 12 months after infusion. Our study shows that selection of the epitope targeting CD30 and ex vivo preservation of less-differentiated memory T cells may enhance the efficacy of CART30 in patients with refractory HL. This trial is registered at www.clinicaltrials.gov (NCT04653649).

Introduction

Hodgkin lymphoma (HL) is 1 of the most curable hematological tumors, but 20% of patients have poor prognosis despite novel therapies.[1,2] HL tumor cells are surrounded by a immunosuppressive microenvironment and yet remain sensitive to immunotherapy (eg, anti-CD30 and anti–programmed cell death protein 1 [PD-1] antibodies).[3,4] T-cell lymphomas represent a heterogeneous group of diseases accounting for 10% to 15% of all non-Hodgkin lymphoma (NHL) cases, showing a poor prognosis with a median 5-year survival rate <30%.[5,6] Chimeric antigen receptor T-cell (CART) therapy directed against CD30 has been explored for patients with relapsed/refractory HL, anaplastic large-cell lymphoma, and CD30$^+$ peripheral T-cell lymphomas.[7-10] CD30 has restricted expression in normal tissues, thus representing an ideal target for HL and CD30$^+$ T-cell NHL (T-NHL) cellular therapies.[11,12] Studies with CD30-directed CART therapy (CART30) in patients with HL revealed a low toxicity profile,[8,9] but despite achieving complete remissions (CRs), most patients relapse while retaining CD30 expression on tumor cells, suggesting that other factors different from antigen escape are limiting the efficacy. Thus, novel strategies should be implemented to improve clinical efficacy of CART30.

CAR design and the targeted epitope location have been associated with CART efficacy.[13] We showed that a second-generation CAR30-4.1BB, targeting a membrane-proximal epitope within the nonsoluble part of CD30, prevents CART blockade and improved antitumor efficacy.[14,15]

Clinical experience with CART19 has unveiled factors associated with effectiveness,[16] including CART products enriched in less-differentiated memory T cells (ie, memory stem [T_{SCM}]) to achieve long-term responses.[17-19] Manufacturing strategies that increase T_{SCM} cells within the infusion products (IPs) would open possibilities for improving CART efficacy. CART manufacturing mostly relies on interleukin-2 (IL-2) or IL-7 with IL-15 for ex vivo T-cell expansion.[20,21] IL-7 and IL-15 promote expansion of memory T cells, but CAR30 products manufactured under these conditions still contain a large proportion of differentiated T cells.[7-9,21]

IL-21 is a cytokine with effects on T, B, and natural killer (NK) T cells, that promotes T-cell memory formation.[22,23] IL-21, with IL-7 and IL-15, enhances CD8 T-cell expansion with preservation of T stem cell memory (T_{SCM}).[22] T cells cultured under IL-21 display longer persistence and enhanced in vivo antitumor effect in preclinical models, which has also been shown with CAR19 T cells.[24] We showed that adding IL-21 to IL-7 and IL-15, together with a short-time CD3/CD28 T-cell activation, increases the proportion of T_{SCM}.[14]

We describe an autologous CAR30 T-cell product, HSP-CAR30, manufactured under novel conditions that significantly increase the proportion of less-differentiated $CAR30^+$ memory T cells. HSP-CAR30 was used to treat patients with $CD30^+$ lymphoma, demonstrating a favorable safety profile and durable complete responses in heavily pretreated patients with HL.

Materials and methods

Study design

This is a single-center phase 1 clinical trial assessing the feasibility and safety of HSP-CAR30, an academic autologous CART30, in adult patients with relapsed/refractory HL and $CD30^+$ T-NHL. The study was registered in the European Union Drug Regulating Authorities Clinical Trials Database (EudraCT 2019-001263-70). Written informed consent was obtained from all patients in accordance with the Declaration of Helsinki. Data monitoring was conducted by Sant Pau's Research Institute Data Safety Monitoring Committee. The clinical trial scheme is described in supplemental Figure 1, available on the *Blood* website. Information regarding eligibility criteria can be found in supplemental Tables 1 and 2.

Phase 1 was conducted between October 2020 and December 2021, with a 3 + 3 design, and dose-limiting toxicities (DLTs) were evaluated to determine the maximum tolerated dose. Three cell dose levels (DLs) were assessed in 3 cohorts: DL1 (3×10^6 $CAR30^+$ T cells/kg), DL2 (5×10^6 $CAR30^+$ T cells/kg), and DL3 (10×10^6 $CAR30^+$ T cells/kg). Patients were enrolled with a 30-day period between them to assess for adverse effects. Secondary end points included clinical efficacy, kinetics of $CAR30^+$ T cells, and survival. DLTs were defined as any of the following toxicities within 30 days of infusion: grade 4 cytokine-release syndrome (CRS), grade 3 CRS unresponsive to corticosteroids and tocilizumab, greater than grade 3 immune effector cell–associated neurotoxicity syndrome (ICANS), and grade 4 liver toxicity without improvement to lower grade within 14 days. Infusion-related toxicities and hematological toxicities were recorded but not considered as DLTs.

Response assessment

Clinical response was evaluated by ^{18}fluorodeoxyglucose–positron emission tomography and contrasted-enhanced computed tomography and assessed according to International Working Group Consensus Response Evaluation Criteria in Lymphoma (2017).[25] Overall response rate was defined as the proportion of patients with CR and partial response (PR). Disease assessment was performed at screening and 1, 3, 6, 12, 18, and 24 months after infusion.

Toxicity assessment

Adverse events were recorded for all treated patients until disease relapse or death, using the Common Terminology Criteria for Adverse Events (version 4.0).[26] CRS and ICANS were graded according to the American Society for Transplantation and Cellular Therapy criteria.[27]

HSP-CAR30 cell manufacturing

HSP-CAR30 IPs were manufactured at the IIB-Sant Pau Research Institute cell facility, in compliance with Good Manufacture Practices, using CliniMACS Prodigy (Miltenyi Biotec, Bergisch Gladbach, Germany) (Figure 1). On day 0, $CD4^+$ and $CD8^+$ T cells (starting material [SM]) positively selected from a fresh leukapheresis, using anti-CD4 and anti-CD8 (CliniMACS CD4 Product Line and CD8 Product Line), were activated with anti-CD3/CD28 (MACS GMP T Cell TransAct) and cultured in human serum-free TexMACS GMP Medium supplemented with IL-7, IL-15, and IL-21 (all from Miltenyi Biotec). On day 1, T cells were transduced with a third-generation lentiviral vector encoding a second-generation CAR30,[15] at a multiplicity of infection of 5. CAR30 T cells were expanded until day 10. IPs were adjusted to the corresponding cohort dose and infused fresh.

Procedures for HSP-CAR30 treatment

supplemental Figure 2 summarizes patient journey from enrollment to HSP-CAR30 infusion. After a screening period of 30 days, patients who met inclusion criteria underwent leukapheresis. Patients received lymphodepleting chemotherapy (LD) with fludarabine, 30 mg/m^2, and bendamustine, 90 mg/m^2 (Flu/Ben), both on days −5 to −3. Ben was replaced with cyclophosphamide, 500 mg/m^2 (Cy/Flu), in patients with T-NHL or those with contraindications to receive Ben. No bridging therapy was allowed. Dose escalations were conducted by consecutive patients, irrespective of disease type. Data were locked as of 31 May 2024.

Real-time quantitative polymerase chain reaction

Genomic DNA (gDNA) was obtained using a PureLink Genomic DNA Mini Kit (Invitrogen, Thermo Fisher Scientific, Waltham, MA), following manufacturer's instructions. Quantitative real-time polymerase chain reaction (PCR) was performed using human RNase P as an endogenous control (2 copies/cell) and the woodchuck hepatitis virus posttranscriptional regulatory element (wpre) as a subrogate gene to detect CAR integration (both from Thermo Fisher Scientific). Further information appears in supplemental Methods 1.

HSP-CAR30 pharmacokinetics studies

C_{max} was defined as the maximum number of copies of wpre/µg gDNA, detected over time (T_{max}). The half-life of HSP-CAR30 was

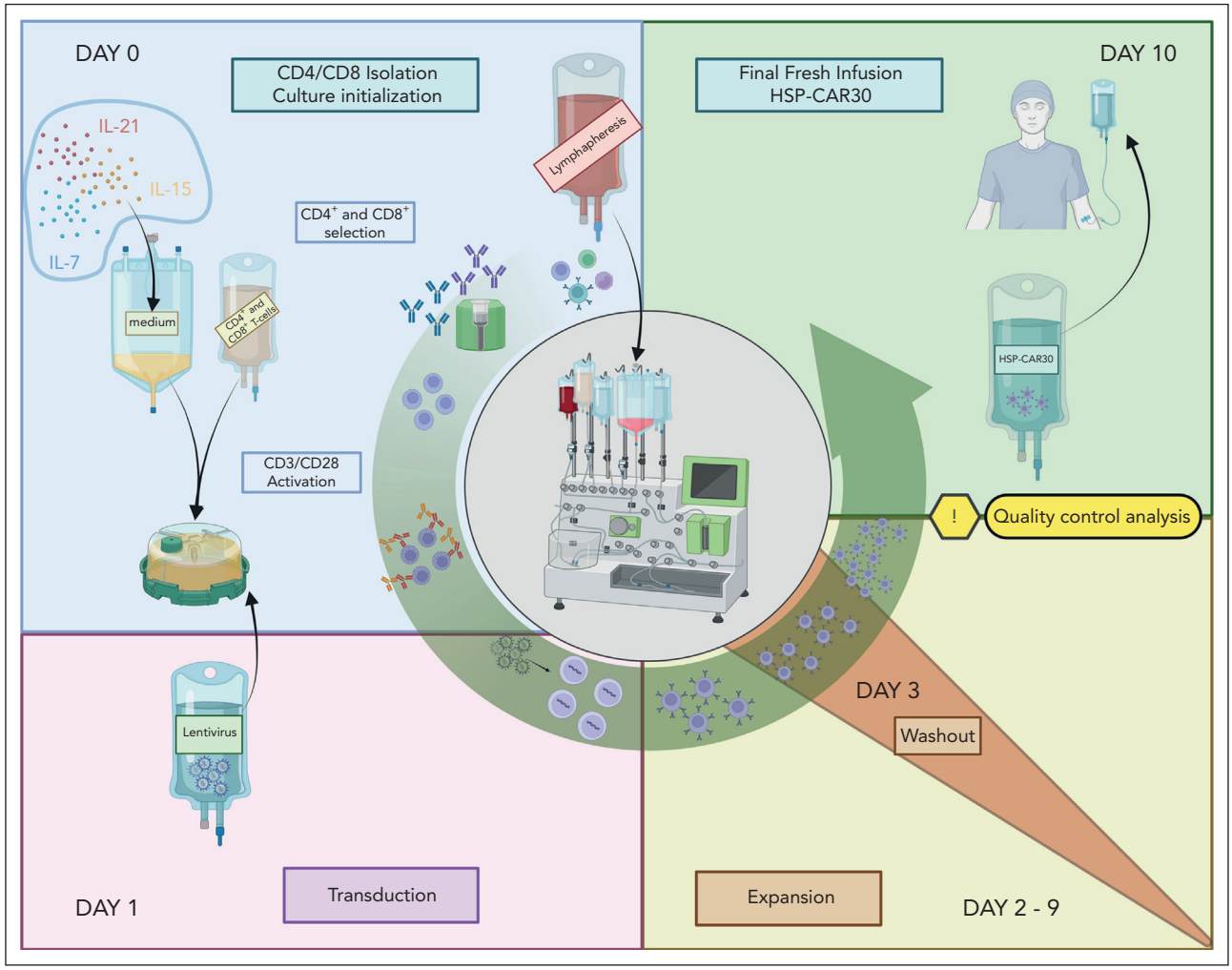

Figure 1. HSP-CAR30 manufacturing process. HSP-CAR30 cell manufacturing was perfomed in closed system CliniMACS Prodigy according to the following steps: in day 0, CD4 and CD8 T cells were isolated from a fresh leukapheresis using anti-CD4/CD8 antibodies. Selected T cells were activated with CD3/CD28 beads and cultured with IL-7, IL-15, and IL-21 cytokines. At day 1, activated T cells were transduced with a third-generation lentiviral vector encoding a second-generation CAR30 at a multiplicity of infection of 5. CD3/CD28 activation was removed at day 3, and CAR30 T cells were expanded until day 10. HSP-CAR30 final product was adjusted to the corresponding cohort dose and freshly infused after lymphodepleting chemotherapy.

defined as the time required for HSP-CAR30 to decrease to half the C_{max}. Time elapsed from the infusion to the last detection of CAR30 T cells by quantitative PCR was used to evaluate the persistence of HSP-CAR30. The area under the curve (AUC) after HSP-CAR30 infusion was calculated following the trapezoidal rule using the AUC function from DescTools R package (version 0.99.54). AUC was calculated from day 0 to T_{max} ($AUC_{0\text{-}Tmax}$).

Cytokines

Serum samples were centrifuged at 3000 rpm for 15 minutes and stored at −80°C. Multiplex assay with Luminex technology was used to analyze interferon gamma, IL-2, IL-6, IL-7, IL-10, IL-12, IL-15, monocyte chemoattractant protein-1, and macrophage inflammatory protein-1β (Milliplex, Merck Life Science, Germany).

RNA-sequencing workflow and differential expression analysis techniques

RNA from SM and IP was sequenced using Illumina technology with the Illumina TruSeq Sample Prep Kit, on a NovaSeq 6000 Sequencing System (Illumina). Nextflow[28] (version 21.04.01) was used to perform the RNA-sequencing (RNA-seq) analysis, using the nf-core/RNA-seq pipeline (version 3.0). STAR (version 2.7.10a) was used for alignment tool, whereas Salmon (version 1.10) was used to quantify the sequenced 100-bp long paired-end reads. These reads were mapped to the GRCh38 reference genome, with the predefined ENSEMBL annotation[29] used to define the aligned transcripts. Detailed information appears in supplemental Methods 2.

Flow cytometry

CAR30 expression was detected by flow cytometry using Alexa Fluor 647–labeled anti–truncated epidermal growth factor receptor (EGFRt) antibody (cetuximab; Roche, Basel, Switzerland). HSP-CAR30 analysis, CAR T-cell in vivo monitoring, and T-cell characterization were analyzed using antibodies described in supplemental Methods 3 and supplemental Table 3. The flow cytometry gating strategy is extensively described in supplemental Figure 3. Briefly, after gating on $CD4^+$ and $CD8^+$ cells, $CCR7^+CD45RO^-$ population was identified and

Table 1. Demographic characteristics and baseline disease features

Characteristic	HSP-CAR30-01	HSP-CAR30-02	HSP-CAR30-03	HSP-CAR30-04	HSP-CAR30-05	HSP-CAR30-06	HSP-CAR30-07	HSP-CAR30-08	HSP-CAR30-09	HSP-CAR30-10	HSP-CAR30-11
Cohort	NI	DL1			DL2			DL3			
Sex	M	M	F	M	M	M	M	M	M	M	M
Age, y	38	42	65	49	48	43	38	63	65	65	21
Diagnosis	cHL	cHL	T-NHL	cHL	cHL	cHL	cHL	cHL	T-NHL	cHL	cHL
Subtype	NS	NS	PTCL-NOS	NS	NS	MC	NS	NS	ALK (–) ALCL	NS	NS
Stage*	IIA	IVA	IVA	IIA	IIA	IVA	IVB	IVA	IVA	IVA	IIIA
Extranodal sites*	—	SC tissue Muscle Bone	Stomach Lung	—	—	Bone Lung	Bone	Bone	Skin SC tissue Muscle	Bone	—
No. of prior lines	11	4	7	5	4	5	4	5	3	5	4
Prior ASCT	Yes	No	Yes	Yes	Yes	No	No	No	Yes	Yes	Yes
ASCT conditioning	BEAM	—	BEAM	BEAM	BEAM	—	—	—	BEAM	BEAM	BEAM
Refractory to BV	Yes	Yes	Yes	No	No	Yes	Yes	Yes	Yes	Yes	No
Refractory to anti–PD-1	No	Yes	Yes	Yes	No	Yes	Yes	Yes	—	No	Yes
Refractory to last treatment	Yes	Yes	Yes	Yes	No	Yes	Yes	Yes	Yes	No	Yes

ALK (–) ALCL, ALK-negative anaplastic large-cell lymphoma; ASCT, autologous stem cell transplantation; BEAM, BCNU, etoposide, cytarabine, melphalan; BV, brentuximab vedotin; cHL, classic Hodgkin lymphoma; F, female; M, male; MC, mixed cellularity; NI, not infused; NS, nodular sclerosis; PTCL-NOS, peripheral T-cell lymphoma not otherwise specified; SC, subcutaneous.

*Disease features at the time of HSP-CAR30 treatment.

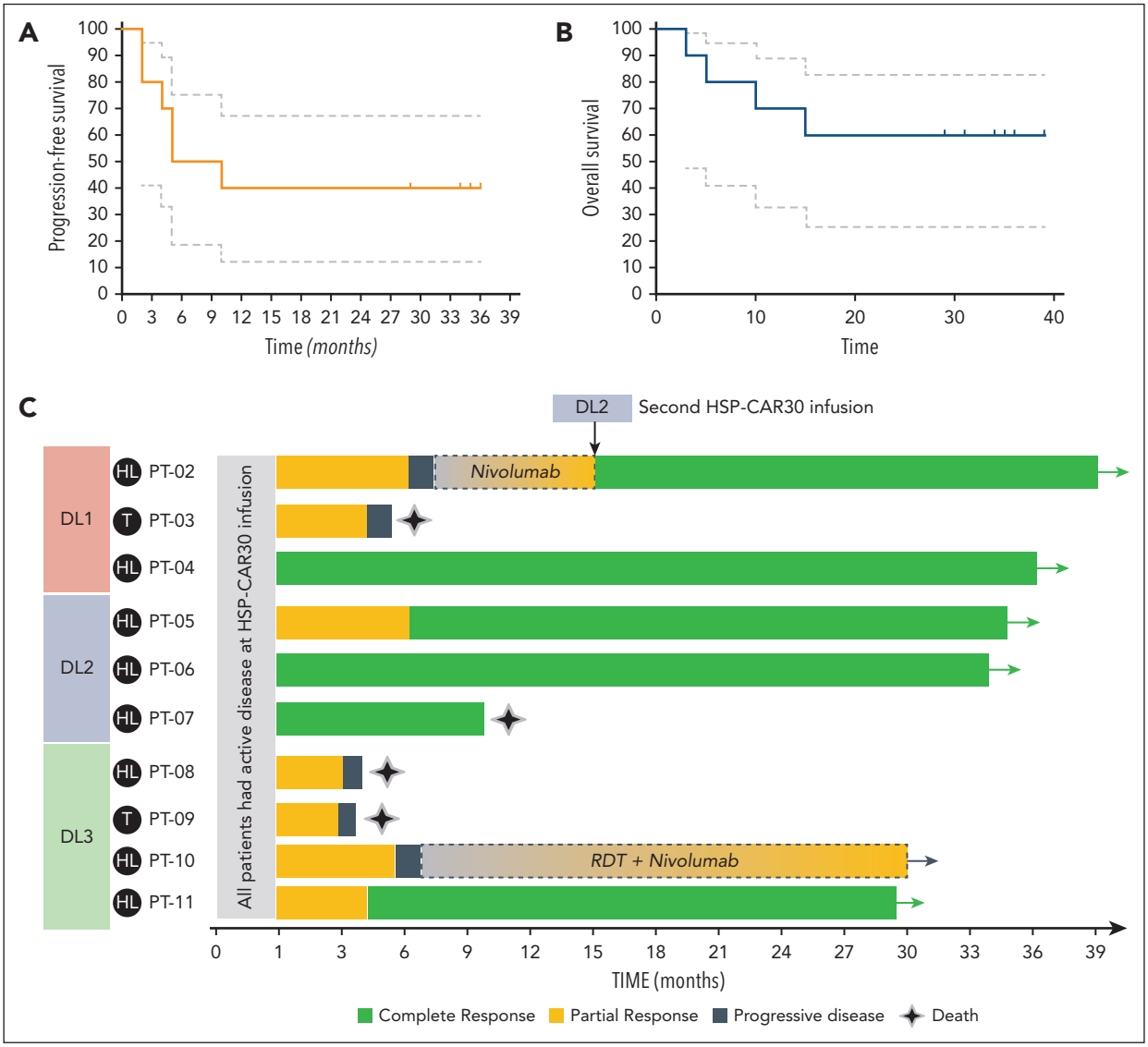

Figure 2. Clinical outcome of patients receiving HSP-CAR30 in the phase 1 clinical trial. (A) Progression-free survival curve. (B) Overall survival curve. (C) Swimmer plot of clinical responses after HSP-CAR30. Patient 02 (PT-02), DL1, presented disease progression and received nivolumab as salvage treatment, achieving PR, and subsequently was treated with a second HSP-CAR30 infusion (DL2: 5×10^6 CAR30$^+$ T cells/kg), achieving an ongoing CR (+22 months). Patient 10 (PT-10), DL3, experienced localized disease progression and received targeted radiotherapy (RDT). Later on, the patient had systemic disease progression, and nivolumab was started, achieving a partial response that is ongoing at last follow-up.

analyzed for CD45RA and CD27. T naïve (T_N) and T_{SCM} were discriminated on the basis of CD95 expression,[30] with T_N being defined as CCR7$^+$CD45RO$^-$CD45RA$^+$CD27$^+$CD95$^-$ and T_{SCM} being defined as CCR7$^+$CD45RO$^-$CD45RA$^+$CD27$^+$CD95$^+$. Central memory CAR30$^+$ T cells (T_{CM}) were CCR7$^+$CD45RO$^+$CD45RA$^-$CD27$^+$CD95$^+$, and T effector memory (T_{EM}) were classified as CCR7$^-$CD45RO$^+$. In the IP, $T_{SCM\text{-}like}$ were identified as CCR7$^+$CD45RO$^+$CD45RA$^+$CD27$^+$CD95$^+$. These analyses were performed according to previous studies that have specifically described the phenotype of T subpopulations.[30-34]

Statistical analysis

Descriptive statistics were measured by mean and range for continuous variables. Categorical data, presented as frequencies and percentages, were used for demographic and baseline characteristics, efficacy, safety, and cellular kinetic/pharmacokinetic measurements. Progression-free survival (PFS) was defined as the time from HSP-CAR30 infusion until documentation of disease progression or death. Overall survival (OS) was measured from the infusion date until death. Patients were censored at the time of last follow-up. PFS and OS were estimated using the Kaplan-Meier method. Analytical statistics were described as mean ± standard error of the mean. Unpaired *t*-tests were used to analyze data from in vitro experiments. $P < .05$ was considered statistically significant. Statistical analyses were performed with IBM SPSS statistical software version 26.0.01 (IBM Corporation, Armonk, NY), R, and GraphPad Prism 6 (GraphPad Software Inc, CA).

Results

Patient characteristics

From October 2020 to December 2021, 11 patients were included in phase 1. The first patient did not receive

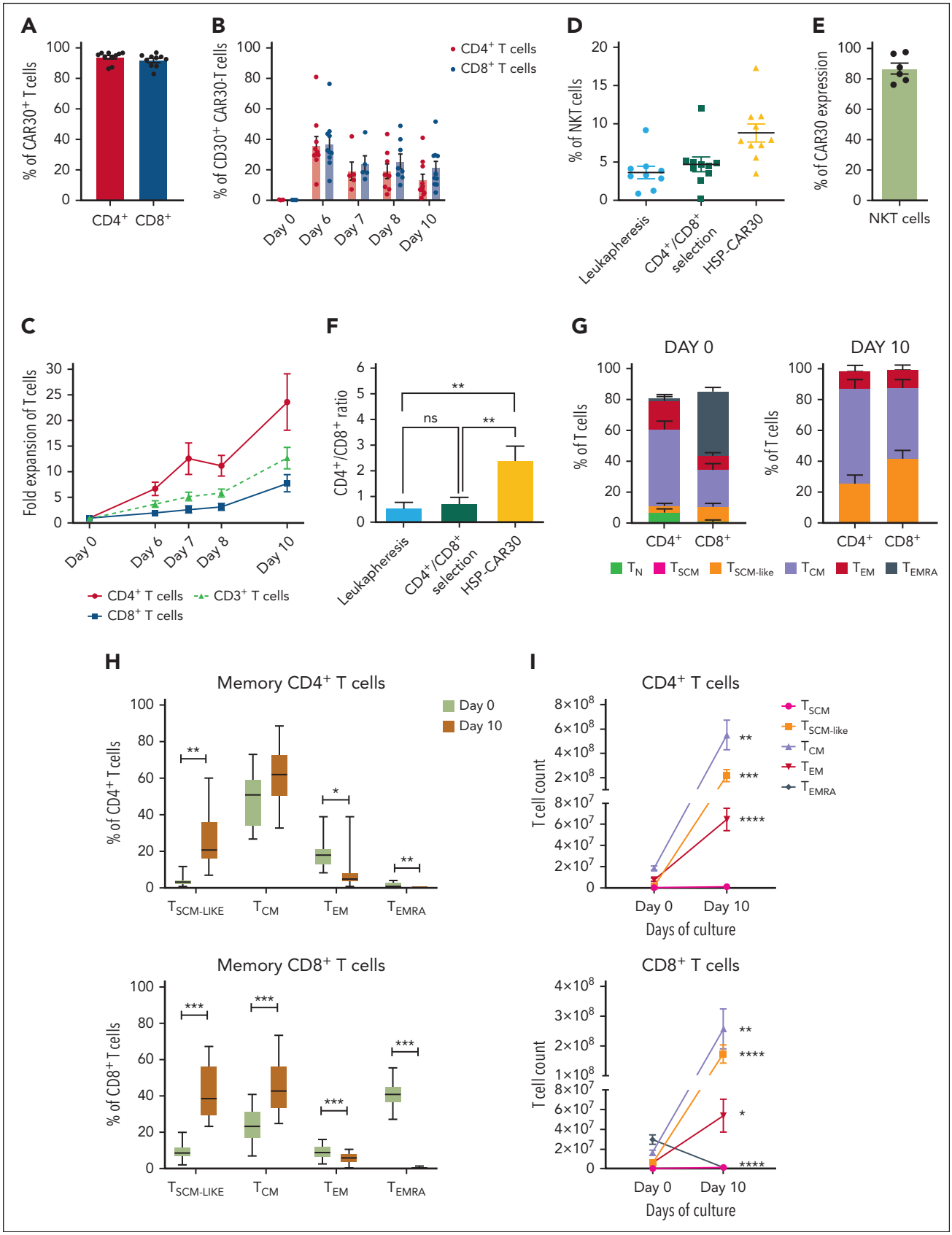

Figure 3. HSP-CAR30 product characterization. HSP-CAR30 products are enriched in CAR30$^+$ cells, with a high proportion of T_{CM} and $T_{SCM\text{-}like}$ memory T cells. (A) CAR30 is highly expressed both in CD4 and CD8 T cells in all final products (n = 10). (B) CD30 protein expression on CD4 (red dots) and CD8 (blue dots) T cells during the culture (day 0, 6, 7, 8 and 10; n = 10). (C) Global fold expansion of manufactured HSP-CAR30 from day 0 to day 10 (CD4, red line; CD8, blue line; CD3, dotted green line) (n = 10). (D) NK T-cell enrichment from day 0 to day 10 (HSP-CAR30 product; n = 10). (E) CAR30 expression on NK T cells at the end of culture (n = 6). NK T cells were gated as CD3$^+$CD56$^+$ cells.

HSP-CAR30 because of production failure due to lack of T-cell expansion, and was discontinued. Ten patients (8 with HL and 2 with CD30$^+$ T-NHL) received treatment according to the protocol. All infused patients had positron emission tomography and contrasted-enhanced computed tomography measurable disease at the time of HSP-CAR30 infusion. Demographic and baseline disease features are summarized in Table 1. Median age was 50 years (range, 21-65 years). Patients had a median number of prior lines of 5 (range, 3–7). Eight of 10 patients (80%) were refractory to the last treatment, and 60% received autologous hemopoietic stem cell transplantation (Table 1). A description of treatments received and responses is provided in supplemental Table 4. All patients received brentuximab vedotin, and 70% were refractory, including 63% of patients with HL and 2 patients with CD30$^+$ T-NHL. Furthermore, 78% of patients with HL were refractory to anti–PD-1 antibodies. The median time from the last therapy to infusion was 3 months (range, 1-6 months). Vein-to-vein time (from apheresis to infusion) was 11 days in all patients. All patients with HL received LD with Flu/Ben, except 1 with a history of a Ben-related skin rash who received Cy/Flu.

Safety of HSP-CAR30 administration

HSP-CAR30 was well tolerated with no DLTs. Grade 1 CRS was observed in 60% of patients, including 4 patients with HL and 2 patients with T-NHL. CRS did not require specific treatment. The median time to CRS onset was 1 day (range, 1-21 days), and the mean duration was 2 days (range, 1-3 days). No patient developed ICANS. A maculopapular skin rash was noted in 4 patients (40%), including both patients with T-NHL. The mean body surface involvement was 31.5% (range, 18%-45%). Skin rash was self-limited in 3 cases but required topical corticosteroids in 1 (supplemental Table 5).

Five patients (50%) developed an infectious episode, mainly viral respiratory infections; most of them occurred >1 month after infusion, and all patients had complete recovery. Three patients (30%) developed (grade ≥3) infections (supplemental Table 6). Hematological toxicity was observed in 8 patients (80%). Prolonged cytopenias (ie, those >3 months) occurred in 2 patients (20%). One patient (PT-11) had grade 3 anemia and grade 4 thrombocytopenia that recovered 5 months after infusion. A second patient (PT-07) had prolonged grade 4 anemia and thrombopenia. A marrow biopsy showed therapy-related acute myeloid leukemia[35] with a complex and monosomic karyotype and *TP53* deletion that resulted in death, unrelated to HSP-CAR30. Three patients died because of disease progression. No other nonrelapse mortality was seen.

Cytokine secretion after HSP-CAR30 infusion

Serum cytokine concentration after HSP-CAR30 infusion showed an overall increase of IL-7 (12.7 ± 3 vs 18.8 ± 3.2 pg/mL), interferon gamma (5.27 ± 1.8 vs 18.06 ± 6 pg/mL; $P < .05$), IL-15 (12.9 ± 9.4 vs 39.0 ± 13.2 pg/mL; $P < .05$), and macrophage inflammatory protein-1β (84.98 ± 30.84 vs 181.0 ± 76.18 pg/mL) (basal vs maximum, respectively) (supplemental Figure 4). Among 6 patients developing CRS, 4 had mild IL-6 elevations (457.3± 339.5 pg/mL). No increases were detected for IL-2, IL-12, and monocyte chemoattractant protein-1 (data not shown).

Immune reconstitution following HSP-CAR30

Rapid recovery of neutrophil counts (without growth factors) was observed after treatment (supplemental Figure 5A). Mean time to B-cell recovery was 128 ± 35 days (supplemental Figure 5B), and levels of immunoglobulins remained stable after treatment (supplemental Figure 5C). Time to NK cell recovery was 25.4 ± 9 days (supplemental Figure 5D). Pre-infusion T cells had an inverted CD4:CD8 ratio (supplemental Figure 5E-G) but, after infusion, there was an increase in CD8$^+$ T cells that was maintained after 1 year. CD4$^+$ T-cell counts were low for up to 6 months, with a time to reach ≥200 CD4$^+$ T cells/μL of 168 ± 54 days (supplemental Figure 5E,G).

HSP-CAR30 displayed specific antitumor efficacy in highly refractory patients

The overall response rate was 100%, including 3 (30%) patients who achieved CR and 7 (70%) of them who reached PR at the first assessment (month 1). PT-05 converted from PR to CR 6 months after infusion, and PT-11 had initially PR and achieved CR 3 months after HSP-CAR30 treatment. Overall CR rate was 50%. All patients with CR had HL, including 1 patient who received DL1, 3 DL2, and 1 DL3. Mean follow-up for alive patients was 34 ± 1.5 months (range, 29-39 months). Two-year PFS and OS were 40% and 60%, respectively (Figure 2A-B). Three patients with HL and 2 with T-NHL had progressive disease after achieving PR (Figure 2C), with a mean time to progression of 3.6 ± 0.68 months (range, 2-5 months). Disease progression was detected in a patient with HL (PT-02) 6 months after receiving DL1 HSP-CAR30. He was treated with nivolumab, achieving PR, and a second HSP-CAR30 infusion (DL2: 5 × 10^6 CAR30$^+$ T cells/kg) was given after LD with Cy/Flu under compassionate use. The patient achieved CR that is ongoing (+22 months). No relapses were seen in patients achieving CR, with a mean CR duration of 33.5 ± 1.55 months (range, 29-36 months).

HSP-CAR30 manufacturing and infusion product characterization

T cells represented 90.4% ± 1.3% of total cells in the IP (supplemental Figure 6A) and had a CAR30 expression of 94.8% ± 1.1% of T cells (93.9% ± 1.2% of CD4$^+$ and 91.9% ± 1.3% of CD8$^+$ T cells) (Figure 3A; supplemental Figure 6B). CD30 expression represented a low proportion of CD4$^+$ (10.1% ± 2.7%) and CD8$^+$ (18% ± 3.1%) T cells (Figure 3B). IPs showed high viability, high overall expansion at the end of culture (23.66 ± 5.48 for CD4$^+$ and 7.78 ± 1.69 for CD8$^+$) (supplemental Figure 6C; Figure 3C), and ex vivo specific antitumor activity against CD30$^+$ tumor cells (supplemental Methods 4;

Figure 3 (continued) (F) CD4 and CD8 T-cell proportion at day 0 after CD4/CD8 selection (green), and HSP-CAR30 final products (yellow) (n = 10). (G) T-cell subpopulations in CD4 and CD8 T cells at day 0 (CD4/CD8 selection) and day 10 of culture (HSP-CAR30 product) (n = 10). Memory T-cell subsets were analyzed using the following markers: CCR7, CD45RO, CD45RA, CD27, and CD95. Subpopulations are defined as follows: T_N (CCR7$^+$CD45RO$^-$CD45RA$^+$CD27$^+$CD95$^-$), T_{SCM} (CCR7$^+$CD45RO$^-$CD45RA$^+$CD27$^+$CD95$^+$), $T_{SCM\text{-}like}$ (CCR7$^+$CD45RO$^+$CD45RA$^+$CD27$^+$CD95$^+$), T_{CM} (CCR7$^+$CD45RO$^+$CD45RA$^-$CD27$^+$CD95$^+$), T_{EM} (CCR7$^-$CD45RO$^+$), and T_{EMRA} (CCR7$^-$CD45RO$^-$). (H) Enrichment of $T_{SCM\text{-}like}$, both in CD4 and CD8, and increase of CD8 T_{CM}-cell population with significant reduction of T_{EM} and T_{EMRA} in HSP-CAR30 products (n = 10). (I) Memory T-cell expansion during HSP-CAR30 manufacturing process (n = 10). All data are represented as mean ± standard error of the mean. Statistical analysis is shown as *$P < .5$; **$P < .1$; ***$P < .01$; ****$P < .001$.

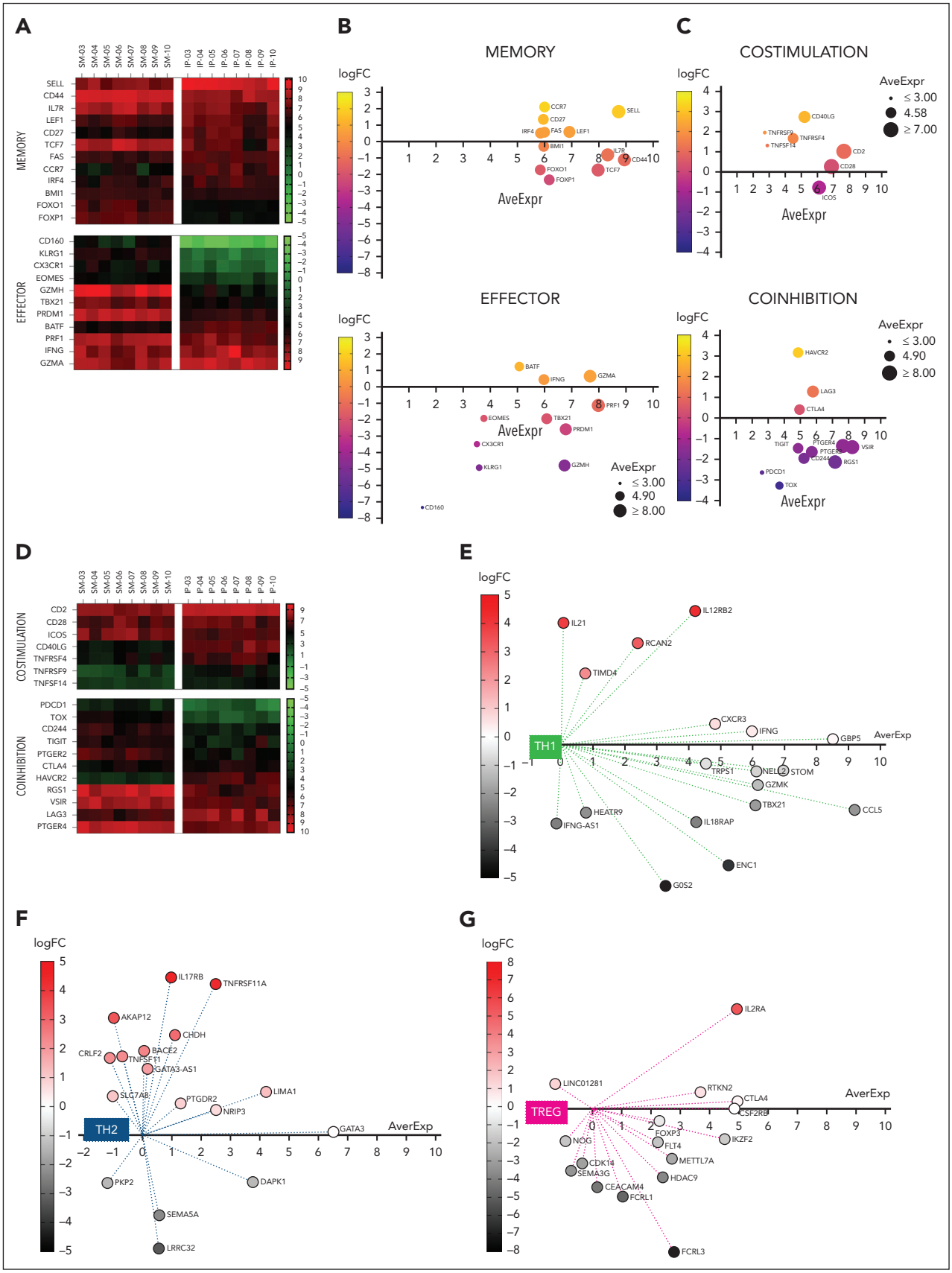

Figure 4. Transcriptome analysis of HSP-CAR30 products. Gene expression levels by RNA-seq analysis were performed to further charactherize HSP-CAR30 products (n = 8). In addition, the differential expression between the IP and SM was analyzed by determining the log-fold change (logFC) for each gene between them. (A) The heat map evidences the high average expression (AveExpr) of all memory-related genes in the IP. (B) Overexpression of memory-related genes in IP compared with SM,

supplemental Figure 6F). NK T cells were also expanded ex vivo (1.8 ± 0.2-fold expansion) (Figure 3D), with most expressing CAR30 (86.7% ± 3.6%) (Figure 3E).

SMs were composed of a high percentage of $CD8^+$ T cells, whereas IP showed a predominance of $CD4^+$ T cells (CD4/CD8 ratio: 0.73 ± 0.24 vs 2.43 ± 0.54, respectively; $P = .0098$) (Figure 3F; supplemental Table 7).

HSP-CAR30 had predominantly memory T cells (90%) (Figure 3G). $CD4^+$ T cells were mainly composed of T_{CM} (61.4% ± 5.09%) and $T_{SCM\text{-}like}$ (25.95% ± 5.06%). $T_{SCM\text{-}like}$ and T_{CM} were the most prevalent subpopulations within $CD8^+$ T cells (41.6% ± 5% and 45.7% ± 5.1%, respectively), whereas T_{EM} and terminal effector memory (T_{EMRA}) represented a low proportion (5.68% ± 1% and 0.2% ± 0.1%, respectively) (Figure 3G). A strong enrichment of $T_{SCM\text{-}like}$ was observed in the IP compared with the SM in $CD4^+$ T cells ($P < .005$) (Figure 3H). Changes in $CD8^+$ T cells were remarkable, with an increase of T_{CM} and $T_{SCM\text{-}like}$ ($P < .0001$) and a significant reduction of T_{EM} and T_{EMRA} ($P < .0001$) (Figure 3H). Overall, the IP had a 171.7 ± 30.8 and 47.3 ± 11.3-fold increase of $CD4^+$ $T_{SCM\text{-}like}$ and T_{CM} cells, and 40.36 ± 9.5 and 19.0 ± 4.6-fold increase of $CD8^+$ $T_{SCM\text{-}like}$ and T_{CM} cells, respectively (Figure 3I).

RNA-seq analysis of IP confirmed a high expression of T-cell stemness and memory-related genes,[30,36,37] including *SELL*, *CD44*, *IL7R*, *LEF1*, *CD27*, *TCF7*, *FAS*, *CCR7*, *FOXP1*, and *FOXO1*. Genes associated with differentiation and effector function[30] were mostly downregulated in IP compared with SM, including *PRF1*, *CX3CR1*, *TBX21*, *KLRG1*, *PRDM1*, *EOMES*, *CD160*, and *GMZH*, although an overexpression of *IFNG* and *GZMA* was found in the IP (Figure 4A-B; supplemental Table 8). IP showed high expression of costimulation genes (*CD40L*, *TNFRSF9* [4-1BB], *TNFRSF4* [OX40], *TNFSF14* [LIGHT], and *CD2*) and downregulation of inhibitory genes,[36-38] some of them associated with a deleterious effect on CAR T cells (*TOX*, *PDCD1* [PD1], *RGS1*, *CD244* [SLAMF4], *PTGER2*, *TIGIT*, *VSIR* [VISTA], and *PTGER4*). In contrast, IP showed an increased expression of *LAG3* and *HAVCR2* (T-cell immunoglobulin mucin receptor 3 [TIM-3]) (Figure 4C-D; supplemental Table 9) that was confirmed by flow cytometry (supplemental Figure 7).

Genetic signatures related to T-helper 1 (Th1), T-helper 2 (Th2), and regulatory T cells (Tregs) were evaluated.[39] *TBX21*, Th1-specific master regulatory transcription factor, maintained a high expression, together with other Th1-associated genes *CXCR3*, *IL12RB2*, *RCAN2*, and *IL21* (Figure 4E; supplemental Table 10). Most of Th2-related genes had lower expression than Th1-associated genes (Figure 4F; supplemental Table 10). Importantly, transcriptome analysis revealed downregulation of most Treg-associated genes[39-41] (Figure 4G; supplemental Table 11).

In vivo HSP-CAR30 T-cell expansion and persistence in peripheral blood

The frequency of $CAR30^+$ T cells at peak of expansion was 18.08% (range, 1.0%-65.3%) (Figure 5A-B) with no differences between doses (Figure 5C). Mean time to $CAR30^+$ T cells peak across all doses was 26.9 days (range, 4-63 days) (Figure 5D). The average number of circulating $CAR30^+$ cells was 172.3 cells/μL (range, 2.3-1051 cells/μL) (Figure 5E).

A preferential increase of $CAR30^+$ $CD8^+$ T cells was observed, although the IP was $CD4^+$ predominant, with a mean $CD4^+/CD8^+$ ratio of 0.73 ± 0.54 (Figure 5F). Remarkably, $CAR30^+$ $CD4^+$ T cells were mostly early-memory T cells, with a predominance of T_{CM} (28.9% ± 4.5%), T_{SCM} (13.4% ± 3.6%), $T_{SCM\text{-}like}$ (4.9% ± 1.4%), and T_N (5.1% ± 1.6%); effector T cells represented a lower proportion that consisted of T_{EM} (29.7% ± 5.1%) and T_{EMRA} (13.2% ± 2.8%) (Figure 5G). $CAR30^+CD8^+$ T cells had a high proportion of less-differentiated memory T cells, with a predominance of T_{SCM} (28.1% ± 3.9%), $T_{SCM\text{-}like}$ (3.2% ± 0.6%), T_N (10.9% ± 1.7%), and T_{CM} cells (9.5% ± 3.6%) (Figure 5G). In contrast, $CAR30^-$ cells consisted mainly of T_{EM} and T_{EMRA} T cells, both in $CD4^+$ (29.7% ± 5.1% and 13.2% ± 2.8%, respectively) and $CD8^+$ T cells (14.4% ± 5.3% and 31.9% ± 3.6%, respectively), with a low proportion of T_{SCM} (4.0% ± 2.0% $CD4^+$ and 4.6% ± 1.0% $CD8^+$), $T_{SCM\text{-}like}$ (0.4% ± 0.1% $CD4^+$ and 3.1% ± 0.6% $CD8^+$), and T_N (1.4% ± 0.7% $CD4^+$ and 2.1% ± 0.5% $CD8^+$) (supplemental Figure 8A). Inhibition markers (PD-1, lymphocyte activating gene 3 [LAG-3], TIM-3, and T-cell immunoreceptor with Ig and ITIM domains [TIGIT]) were almost absent in $CAR30^+$ T cells at peak of expansion (supplemental Figure 8B). Tregs at expansion peak represented 12.2% ± 3.9% of bulk T cells but were negligible (0.46% ± 0.2%) within $CAR30^+$ T cells (supplemental Figure 8C).

Kinetics of $CAR30^+$ T cells assessed by real-time quantitative PCR showed a mean C_{max} of 72 875 ± 27 885 copies of wpre/μg gDNA, with no differences between doses ($P = .52$) (Figure 6A). Mean T_{max} was 20 ± 4.4 days. Mean AUC from day 0 to T_{max} ($AUC_{0\text{-}Tmax}$) was 716 894 ± 254 699 copies of wpre/μg gDNA × days with no differences between doses (Figure 6B-C). C_{max} and $AUC_{0\text{-}Tmax}$ in patients with HL were similar among doses (Figure 6D-E; supplemental Table 12). However, patients with HL achieving CR had a trend to higher $AUC_{0\text{-}Tmax}$ values (828 481 ± 307 082 copies of wpre/μg gDNA × days in CR vs 150 362 ± 101 732 in non-CR patients; $P = .1543$) (Figure 6F).

Long-term persistence of HSP-CAR30 is shown in Figure 6G. $CAR30^+$ T cells were detected in 5 of 7 (71%) evaluable patients 9 months after infusion, and 80% of them were in CR. One year after infusion, $CAR30^+$ T cells remained detectable in 3 of 5 (60%) evaluable patients. $CAR30^+$ T cells were still detected in those patients with the longest follow-up (at 24 months for PT-04, and 21 months for PT-11).

Figure 4 (continued) including *CCR7*, *SELL*, *CD27*, IRF4, *LEF1*, and *FAS*. Effector-associated genes were downregulated in IP compared with SM, but maintained a high expression. (C) Gene expression of costimulatory and inhibitory molecules. Downregulation of gene expression of several inhibition markers with overexpression of HAVCR2 and LAG3. (D) Heat map representing AveExpr of genes linked to costimulatory and coinhibitory molecules. (E) T-helper 1 (Th1) genetic signature in HSP-CAR30 products. Th1-associated genes had high AveExpr, although some were downregulated in the IP. (F) T-helper 2 (Th2) genetic signatures. Th2-related genes were upregulated but remained with a low AveExpr. (G) Genetic signatures of regulatory T cells (Tregs); Treg-associated genes were downregulated in the IP and had a low AveExpr. In heat maps (A,D), red and green colors represented high and low expression, respectively. (B-C,E-G) Bubble plots representing the logFC (y axis) and AveExpr (x axis) of specific genes.

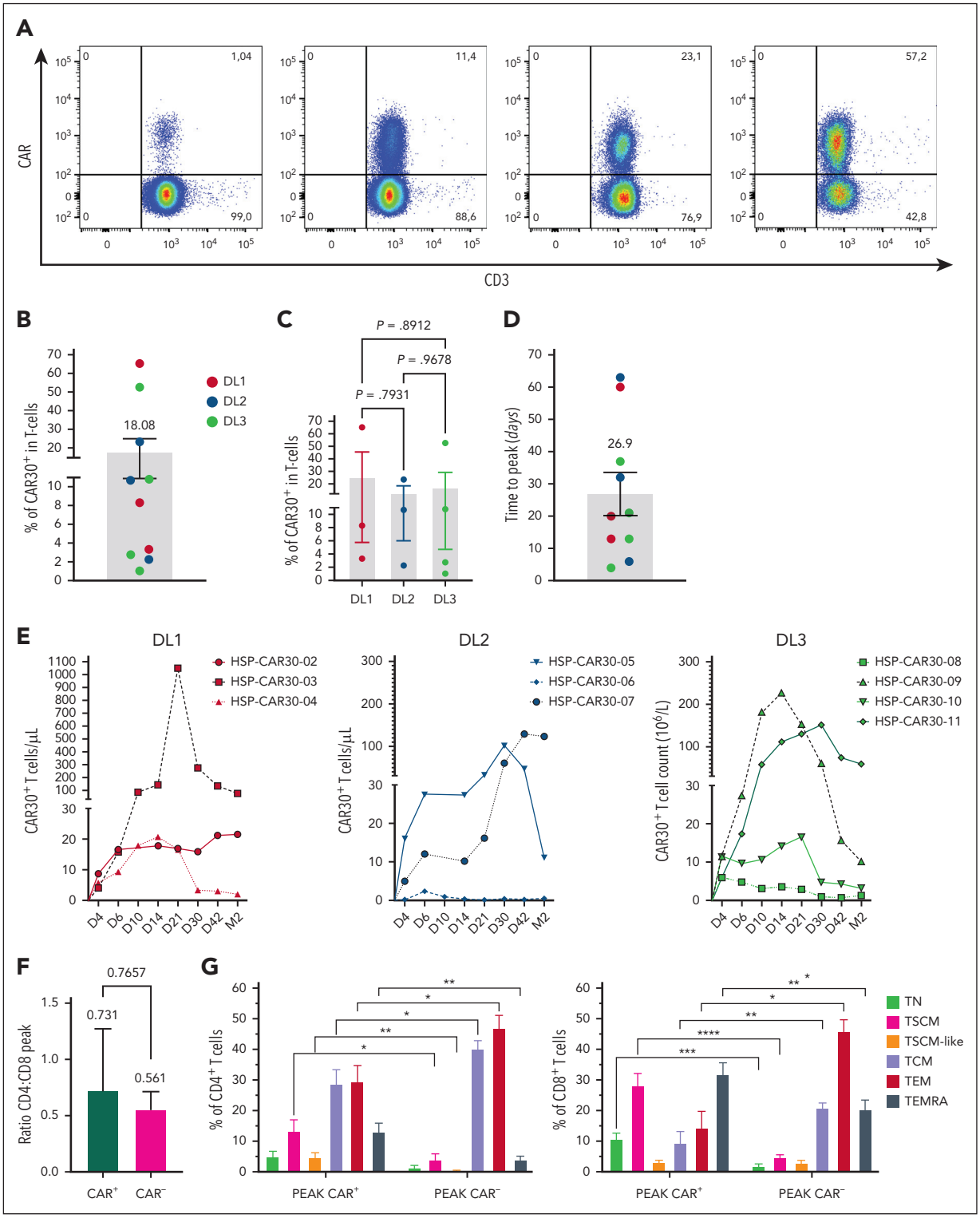

Figure 5. In vivo CAR30$^+$ T-cell expansion after HSP-CAR30 infusion. Samples from all infused patients were analyzed at the expansion peak after HSP-CAR30 infusion. (A) Representative plots of CAR30$^+$ T-cell detection by flow cytometry in peripheral blood of difffeents patients, at distinct times after HSP-CAR30 treatment. (B) Percentage of CAR30$^+$ T cells detected at the expansion peak. (C) Percentage of CAR30$^+$ T cells at peak of expansion across the 3 doses evaluated. Red bars represent DL1, blue bar DL2, and green bar DL3. (D) Time to CAR30$^+$ T-cell peak. (E) CAR30$^+$ T-cell counts over 2 months after HSP-CAR30 infusion for each patient. From left to right, the graphs represent patients in DL1, DL2, and DL3, respectively. (F) CD4/CD8 ratio in CAR$^+$ and CAR$^-$ T cells at peak of T-cell expansion (n = 10). (G) T-cell subpopulations within CAR$^+$ and CAR$^-$ T cells, in CD4 and CD8 T lymphocytes. (B,D) Red dots represent patients in DL1, blue dots patients in DL2, and green dots patients in DL3. All bar graphs are represented as the mean ± standard error of the mean. *P < .05; **P < .01; ***P < .001; ****P < .0001 (n = 10).

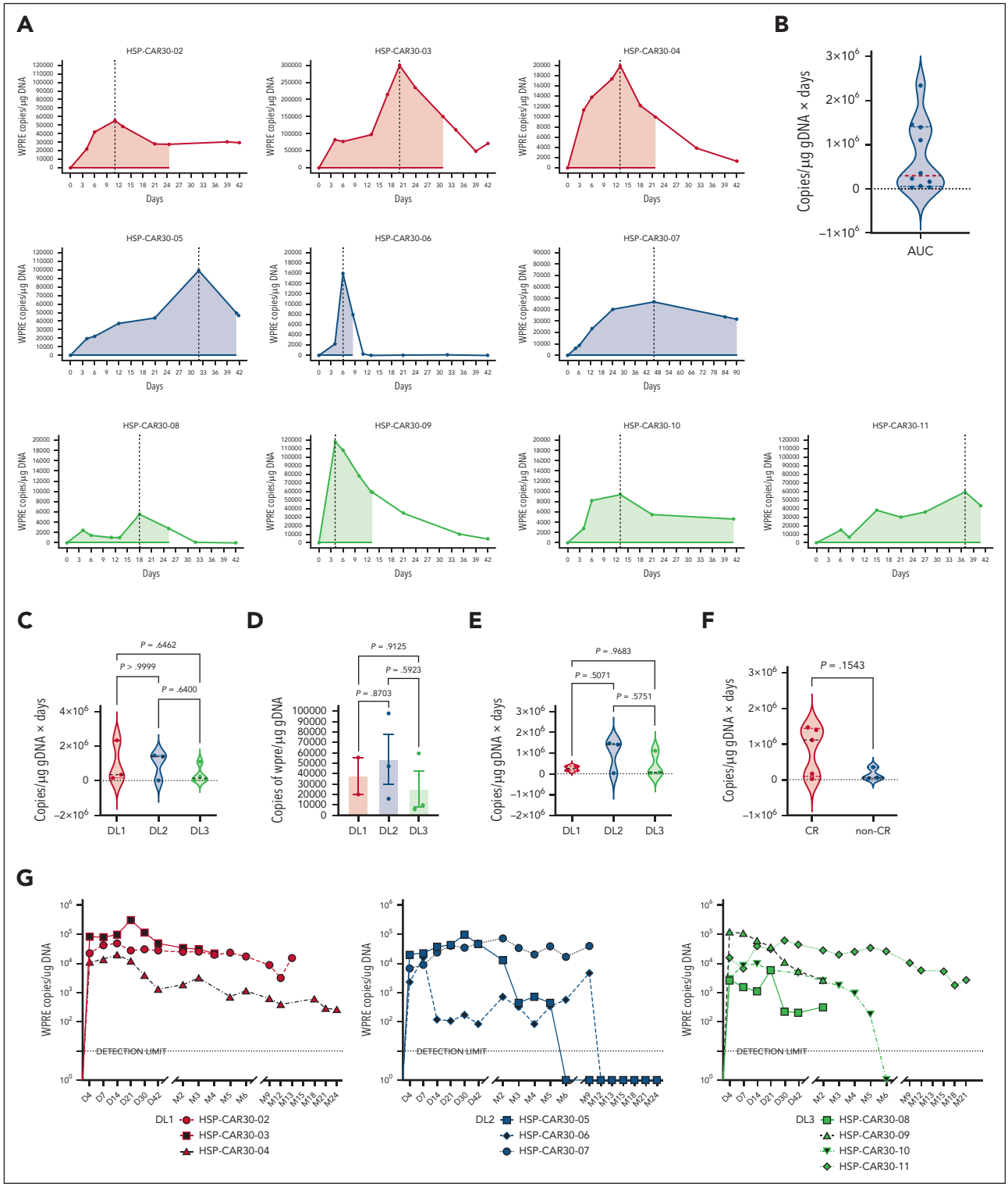

Figure 6. Kinetics of CAR30 detection by real-time quantitative PCR after HSP-CAR30 infusion. (A) Curves represent CAR30 kinetics in peripheral blood after infusion up to day +42, and the maximun wpre/µDNA copy number (C_{max}) for each patient is shown. The red lines represent patients who received DL1, the blue lines DL2, and the green lines DL3. Black dotted lines represent the time to reach C_{max} (T_{max}), whereas the shaded areas represent the half-life of HSP-CAR30 for each patient. (B) The AUC after HSP-CAR30 was calculated from infusion to T_{max}. (C) $AUC_{0\text{-}Tmax}$ was not different between the 3 doses. (D) C_{max} in patients with HL (n = 8); no differences were found between DL1 (red bar), DL2 (blue bar), and DL3 (green bar). (E) $AUC_{0\text{-}Tmax}$ in patients with HL. (F) $AUC_{0\text{-}Tmax}$ in patients with HL who reached CR (red violin plot) vs those who did not achieve CR (blue violin plot); there is a trend toward higher $AUC_{0\text{-}Tmax}$ values in CR patients. (G) Long-term persistence of $CAR30^+$ T cells in vivo in patients receiving DL1 (red), DL2 (blue), and DL3 (green) of HSP-CAR30. (B,C,E,F) Violin plots represents distribution of the data showing all considered values. Dotted lines represent the median value. (D) Bar graphs are represented as the mean ± standard error of the mean.

Discussion

Few clinical trials with CART30 have been conducted in patients with refractory CD30$^+$ hematological malignancies. Although long-term durable responses had been demonstrated, efficacy improvements are needed.[7,8,10]

We report the mature data of the phase 1 study in patients with CD30$^+$ lymphoma, mostly HL, who were refractory to brentuximab and anti–PD-1 therapy. Initial response rate was similar to a previous study.[7] Remarkably, 60% of patients (all with HL) achieved long-term CR, with none of them relapsing after a median follow-up of >2 years. Responses were achieved with a favorable safety profile, which is reflected in the cytokine secretion analysis with low levels of proinflammatory cytokines after HSP-CAR30 infusion. Like previous CART30 studies,[7,8,10] we observed severe cytopenias, mostly due to lymphodepletion. The role of Ben, used in most of our patients, remains to be determined, although recent reports evaluating its use for lymphodepletion of CART patients suggest that it has a favorable safety profile without compromising efficacy.[42]

Preliminary efficacy data are favorable and potentially associated with the strategies implemented to improve CART30 efficacy. Our CAR30 targets an epitope within the proximal region of CD30,[13,43] preventing blockade of CART function by CD30 shedding.[44-46] In addition, we used IL-21 in our manufacturing process to enhance the ex vivo generation of T_{SCM} and T_{CM}.[14,47,48] In fact, the IP had a high proportion of $T_{SCM\text{-}like}$ and T_{CM}, representing >80% of CAR30$^+$ T cells, in contrast to previous CART30 studies where products had a significant proportion of differentiated T cells.[8,9] This suggests an important role of IL-21 in preserving less-differentiated memory T cells,[23,24] together with a short CD3/CD28 activation. Nevertheless, the stimulation of T cells during the manufacturing process may induce expression of T-cell markers to an extent that can make T-cell subset classification a challenge, which requires the use of rigorous protocols for T-cell identification and applying definitions for T-cell subsets of standard use that were previously defined.[30-34] In fact, most T_{SCM} cells found in IP coexpressed CD45RO while maintaining high expression of CD45RA, CCR7, and CD95, a phenotype described as $T_{SCM\text{-}like}$.[14,32]

IP transcriptional studies demonstrated a high gene expression associated to T-cell stemness (*SELL*, *TCF7*, *LEF1*, *FOXP1*, and *FOXO1*).[30,37,49-51] Interestingly, IP had a high expression of *CD2* gene, associated with serial killing.[52] It remains unknown if this impacts on the efficacy of HSP-CAR30, because relapsed patients with HL may have low tumor expression of CD58, the natural ligand of CD2.[53]

The IP had a proportion of T cells expressing inhibitory receptors (PD-1, TIM-3, and LAG-3) that could be related to transient CD30 expression on activated T cells during manufacturing.[14,15] Ex vivo generation of T_{SCM}/T_{CM} CAR T cells may exhibit high expression of inhibitory receptors after tumor antigen exposure, without being functionally exhausted.[54] Furthermore, IP had downregulation of exhaustion-associated genes *TOX*, *PCD1*, *CD244*, and *TIGIT*.[51] Collectively, HSP-CAR30 contains CAR T cells with a gene expression profile that could resemble the recently described "CD8 fit T cells," a mix of cells with effector functionality and long-term persistence, that have been correlated with better outcome.[55]

In vivo studies revealed preponderance of CAR30$^+$CD8$^+$ T cells at expansion peak despite an IP predominance of CAR30$^+$CD4$^+$ T cells. This preferential in vivo expansion of CD8$^+$ T cells has been described for CART19.[56] Analysis of T-cell subsets at expansion peak unveiled that 50% of CAR30$^+$ T cells were early-memory T cells, including a significant proportion (>25%) of T_{SCM}. These data suggest that the high proportion of early memory CAR30$^+$ T cells in the IP contributes to the generation of CAR30$^+$ memory T cells at expansion peak.[18,56,57] In contrast, CART$^-$ cell subsets at the same time point showed a more differentiated phenotype, likely reflecting peripheral blood T-cell composition in heavily treated patients with lymphoma.[58] These observations may be related to the long-term responses detected in our patients.[15,59]

In summary, this phase 1 study demonstrated the safety of HSP-CAR30 with a remarkable proportion of long-term responses, suggesting that infusion of a fresh product and the implementation of manufacturing procedures to enrich for early-memory CART cells (ie, short-term T-cell activation and addition of IL-21 for ex vivo CART expansion), together with targeting CD30 proximal epitopes may translate into improved efficacy. On the basis of favorable safety and preliminary efficacy data, a phase 2 trial is ongoing, focused on patients with HL with DL2 as the selected dose, to allow obtaining the target dose while having significant antitumor activity.

Acknowledgments

This work was supported in part by grants from La Marató TV3 (Exp. 20130710), Josep Carreras Leukemia Research Institute, Instituto de Salud Carlos III (ISCIII Fondo de Investigaciones Sanitarias PI15/1383 and PI18/01023; ICI19/060; European Union), Deutsche José Carreras Leukämie-Stiftung (10R/2016), Fundación "la Caixa," Agència de Gestió d'Ajuts Universitaris i de Recerca (SGR2021/1139) Red de Terapias Avanzadas (Redes de Investigación Cooperativa Orientadas al Resultado en Salud, ISCIII; RD21/0017/0011; Next Generation, European Union), and Banc de Sang i Teixits.

Authorship

Contribution: A.C.C. and J.B. designed the study, led the clinical trial, provided medical care, analyzed data, contributed to data collection for study patients, and wrote the manuscript; C.U.-M. led chimeric antigen receptor T-cell (CART) manufacturing and contributed to data collection, data analysis, and writing of the manuscript; P.P.-F. contributed to CART expansion analysis and studies of CART infusion products; R.M.-T. contributed to CART manufacturing, CART expansion analysis, and cytokine analysis; E.E.-L. contributed to studies of CART infusion products; M.G.-P. and P.J.-B. contributed to data analysis; J.S. contributed to clinical data analysis; E.I. contributed to statistical analysis; I.G.-C., A.E., R.M., M.-E.M.-M., and M.R. contributed to medical care of patients; P.E. and J.M.S. performed RNA-sequencing studies; and C.A.-F. and L.E.-G. led CART manufacturing and quality control of CART infusion products and contributed to data analysis and writing of the manuscript.

Conflict-of-interest disclosure: The authors declare no competing financial interests.

ORCID profiles: A.C.C., 0000-0002-4950-5259; I.G.-C., 0000-0002-2994-9055; A.E., 0000-0002-6062-5980; R.M., 0000-0001-5143-4042; P.E., 0000-0002-5534-5124; M.-E.M.-M., 0000-0001-6752-873X; M.R., 0000-0002-2409-6946; J.S., 0000-0002-7966-0356; J.B., 0000-0003-2750-3735.

Correspondence: Javier Briones, Hematology Service, Hospital Santa Creu i Sant Pau, Mas Casanovas 90, 08041 Barcelona, Spain; email: jbriones@santpau.cat.

Footnotes

Submitted 3 September 2024; accepted 23 December 2024; prepublished online on *Blood* First Edition 22 January 2025. https://doi.org/10.1182/blood.2024026758.

*A.C.C. and C.U.-M. share first authorship.

†C.A.-F., L.E.-G., and J.B. contributed equally to this work and share senior authorship.

Data are available on reasonable request from the corresponding author, Javier Briones (jbriones@santpau.cat).

The online version of this article contains a data supplement.

There is a *Blood* Commentary on this article in this issue.

The publication costs of this article were defrayed in part by page charge payment. Therefore, and solely to indicate this fact, this article is hereby marked "advertisement" in accordance with 18 USC section 1734.

REFERENCES

1. Mohty R, Dulery R, Bazarbachi AH, et al. Latest advances in the management of classical Hodgkin lymphoma: the era of novel therapies. *Blood Cancer J*. 2021;11(7):126.
2. Zhang Y, Xing Z, Mi L, et al. Novel agents for relapsed and refractory classical Hodgkin lymphoma: a review. *Front Oncol*. 2022;12:929012.
3. Chen R, Gopal AK, Smith SE, et al. Five-year survival and durability results of brentuximab vedotin in patients with relapsed or refractory Hodgkin lymphoma. *Blood*. 2016;128(12):1562-1566.
4. Ansell SM, Bröckelmann PJ, von Keudell G, et al. Nivolumab for relapsed/refractory classical Hodgkin lymphoma: 5-year survival from the pivotal phase 2 CheckMate 205 study. *Blood Adv*. 2023;7(20):6266-6274.
5. O'Connor OA, Bhagat G, Ganapathi K, et al. Changing the paradigms of treatment in peripheral T-cell lymphoma: from biology to clinical practice. *Clin Cancer Res*. 2014;20(20):5240-5254.
6. Vose JM, Neumann M, Harris ME. International peripheral T-cell and natural killer/T-cell lymphoma study: pathology findings and clinical outcomes international T-cell lymphoma project. *J Clin Oncol*. 2008;26(25).
7. Ramos CA, Grover NS, Beaven AW, et al. Anti-CD30 CAR-T cell therapy in relapsed and refractory Hodgkin lymphoma. *J Clin Oncol*. 2020;38(32):3794-3804.
8. Wang CM, Wu ZQ, Wang Y, et al. Autologous T cells expressing CD30 chimeric antigen receptors for relapsed or refractory Hodgkin lymphoma: an open-label phase I trial. *Clin Cancer Res*. 2017;23(5):1156-1166.
9. Ramos CA, Ballard B, Zhang H, et al. Clinical and immunological responses after CD30-specific chimeric antigen receptor-redirected lymphocytes. *J Clin Invest*. 2017;127(9):3462-3471.
10. Brudno JN, Natrakul DA, Karrs J, et al. Transient responses and significant toxicities of anti-CD30 CAR T cells for CD30+ lymphomas: results of a phase 1 trial. *Blood Adv*. 2024;8(3):802-814.
11. Horie R, Watanabe T. CD30: expression and function in health and disease. *Semin Immunol*. 1998;10(6):457-470.
12. van der Weyden CA, Pileri SA, Feldman AL, Whisstock J, Prince HM. Understanding CD30 biology and therapeutic targeting: a historical perspective providing insight into future directions. *Blood Cancer J*. 2017;7(9):e603.
13. Haso W, Lee DW, Shah NN, et al. Anti-CD22-chimeric antigen receptors targeting B-cell precursor acute lymphoblastic leukemia. *Blood*. 2013;121(7):1165-1174.
14. Alvarez-Fernández C, Escribà-Garcia L, Vidal S, Sierra J, Briones J. A short CD3/CD28 costimulation combined with IL-21 enhance the generation of human memory stem T cells for adoptive immunotherapy. *J Transl Med*. 2016;14(1):214.
15. Alvarez-Fernández C, Escribà-Garcia L, Caballero AC, et al. Memory stem T cells modified with a redesigned CD30-chimeric antigen receptor show an enhanced antitumor effect in Hodgkin lymphoma. *Clin Transl Immunol*. 2021;10(4):e1268.
16. Caballero AC, Escribà-Garcia L, Alvarez-Fernández C, Briones J. CAR T-cell therapy predictive response markers in diffuse large B-cell lymphoma and therapeutic options after CART19 failure. *Front Immunol*. 2022;13:904497.
17. Fraietta JA, Lacey SF, Orlando EJ, et al. Determinants of response and resistance to CD19 chimeric antigen receptor (CAR) T cell therapy of chronic lymphocytic leukemia. *Nat Med*. 2018;24(5):563-571.
18. Biasco L, Izotova N, Rivat C, et al. Clonal expansion of T memory stem cells determines early anti-leukemic responses and long-term CAR T cell persistence in patients. *Nat Cancer*. 2021;2(6):629-642.
19. Locke FL, Rossi JM, Neelapu SS, et al. Tumor burden, inflammation, and product attributes determine outcomes of axicabtagene ciloleucel in large B-cell lymphoma. *Blood Adv*. 2020;4(19):4898-4911.
20. Ayala Ceja M, Khericha M, Harris CM, Puig-Saus C, Chen YY. CAR-T cell manufacturing: major process parameters and next-generation strategies. *J Exp Med*. 2024;221(2):e20230903.
21. Arcangeli S, Falcone L, Camisa B, et al. Next-generation manufacturing protocols enriching TSCM CAR T cells can overcome disease-specific T cell defects in cancer patients. *Front Immunol*. 2020;11:1217.
22. Spolski R, Leonard WJ. Interleukin-21: a double-edged sword with therapeutic potential. *Nat Rev Drug Discov*. 2014;13(5):379-395.
23. Tian Y, Zajac AJ. IL-21 and T cell differentiation: consider the context. *Trends Immunol*. 2016;37(8):557-568.
24. Singh H, Figliola MJ, Dawson MJ, et al. Reprogramming CD19-specific T cells with IL-21 signaling can improve adoptive immunotherapy of B-lineage malignancies. *Cancer Res*. 2011;71(10):3516-3527.
25. Younes A, Hilden P, Coiffier B, et al. International Working Group consensus response evaluation criteria in lymphoma (RECIL 2017). *Ann Oncol*. 2017;28(7):1436-1447.
26. National Cancer Institute. Common Terminology Criteria for Adverse Events (CTCAE) Version 4.0. NIH Publication; 2009.
27. Lee DW, Santomasso BD, Locke FL, et al. ASTCT consensus grading for cytokine release syndrome and neurologic toxicity associated with immune effector cells. *Biol Blood Marrow Transplant*. 2019;25(4):625-638.
28. Di Tommaso P, Chatzou M, Floden EW, Barja PP, Palumbo E, Notredame C. Nextflow enables reproducible computational workflows. *Nat Biotechnol*. 2017;35(4):316-319.
29. Aken BL, Ayling S, Barrell D, et al. The Ensembl gene annotation system. *Database*. 2016;2016:baw093.
30. Gattinoni L, Lugli E, Ji Y, et al. A human memory T cell subset with stem cell-like properties. *Nat Med*. 2011;17(10):1290-1297.
31. Sabatino M, Hu J, Sommariva M, et al. Generation of clinical-grade CD19-specific CAR-modified CD81 memory stem cells for the treatment of human B-cell malignancies. *Blood*. 2016;128(4):519-528.
32. Cieri N, Camisa B, Cocchiarella F, et al. IL-7 and IL-15 instruct the generation of human memory stem T cells from naive precursors. *Blood*. 2013;121(4):573-584.
33. Gattinoni L, Speiser DE, Lichterfeld M, Bonini C. T memory stem cells in health and disease. *Nat Med*. 2017;23(1):18-27.
34. Lugli E, Gattinoni L, Roberto A, et al. Identification, isolation and in vitro expansion

of human and nonhuman primate T stem cell memory cells. *Nat Protoc*. 2013;8(1):33-42.

35. Arber DA, Orazi A, Hasserjian R, et al. The 2016 revision to the World Health Organization classification of myeloid neoplasms and acute leukemia. *Blood*. 2016; 127(20):2391-2405.

36. Galletti G, De Simone G, Mazza EMC, et al. Two subsets of stem-like CD8+ memory T cell progenitors with distinct fate commitments in humans. *Nat Immunol*. 2020;21(12): 1552-1562.

37. Im SJ, Hashimoto M, Gerner MY, et al. Defining CD8+ T cells that provide the proliferative burst after PD-1 therapy. *Nature*. 2016;537(7620):417-421.

38. Wherry EJ, Ha SJ, Kaech SM, et al. Molecular signature of CD8+ T cell exhaustion during chronic viral infection. *Immunity*. 2007;27(4): 670-684.

39. Radens CM, Blake D, Jewell P, Barash Y, Lynch KW. Meta-analysis of transcriptomic variation in T-cell populations reveals both variable and consistent signatures of gene expression and splicing. *RNA*. 2020;26(10): 1320-1333.

40. Nagata S, Ise T, Pastan I. Fc receptor-like 3 protein expressed on IL-2 nonresponsive subset of human regulatory T cells. *J Immunol*. 2009;182(12):7518-7526.

41. Bhairavabhotla R, Kim YC, Glass DD, et al. Transcriptome profiling of human FoxP3+ regulatory T cells. *Hum Immunol*. 2016;77(2): 201-213.

42. Ghilardi G, Paruzzo L, Svoboda J, et al. Bendamustine lymphodepletion before axicabtagene ciloleucel is safe and associates with reduced inflammatory cytokines. *Blood Adv*. 2024;8(3):653-666.

43. Nagata S, Ise T, Onda M, et al. Cell membrane-specific epitopes on CD30: potentially superior targets for immunotherapy. *Proc Natl Acad Sci U S A*. 2005;102(22):7946-7951.

44. Hansen HP, Recke A, Reineke U, et al. The ectodomain shedding of CD30 is specifically regulated by peptide motifs in its cysteine-rich domains 2 and 5. *Faseb J*. 2004;18(7): 893-895.

45. Josimovic-Alasevic O, Dürkop H, Schwarting R, Backé E, Stein H, Diamantstein T. Ki-1 (CD30) antigen is released by Ki-1-positive tumor cells in vitro and in vivo, I: partial characterization of soluble Ki-1 antigen and detection of the antigen in cell culture supernatants and in serum by an enzyme-linked immunosorbent assay. *Eur J Immunol*. 1989;19(1):157-162.

46. Schirrmann T, Steinwand M, Wezler X, Ten Haaf A, Tur MK, Barth S. CD30 as a therapeutic target for lymphoma. *BioDrugs*. 2014;28(2):181-209.

47. Rochman Y, Spolski R, Leonard WJ. New insights into the regulation of T cells by γc family cytokines. *Nat Rev Immunol*. 2009;9(7): 480-490.

48. Zeng R, Spolski R, Finkelstein SE, et al. Synergy of IL-21 and IL-15 in regulating CD8+ T cell expansion and function. *J Exp Med*. 2005;201(1):139-148.

49. Chan JD, Scheffler CM, Munoz I, et al. FOXO1 enhances CAR T cell stemness, metabolic fitness and efficacy. *Nature*. 2024; 629(8010):201-210.

50. Doan AE, Mueller KP, Chen AY, et al. FOXO1 is a master regulator of memory programming in CAR T cells. *Nature*. 2024; 629(8010):211-218.

51. Zhu Z, Lou G, Teng X-L, et al. FOXP1 and KLF2 reciprocally regulate checkpoints of stem-like to effector transition in CAR T cells. *Nat Immunol*. 2024;25(1):117-128.

52. Romain G, Strati P, Rezvan A, et al. Multidimensional single-cell analysis identifies a role for CD2-CD58 interactions in clinical antitumor T cell responses. *J Clin Invest*. 2022;132(17):e159402.

53. Abdul Razak FR, Diepstra A, Visser L, van den Berg A. CD58 mutations are common in Hodgkin lymphoma cell lines and loss of CD58 expression in tumor cells occurs in Hodgkin lymphoma patients who relapse. *Genes Immun*. 2016;17(6):363-366.

54. Arcangeli S, Bove C, Mezzanotte C, et al. CAR T cell manufacturing from naive/stem memory T lymphocytes enhances antitumor responses while curtailing cytokine release syndrome. *J Clin Invest*. 2022;132(12): e150807.

55. Rezvan A, Romain G, Fathi M, et al. Identification of a clinically efficacious CAR T cell subset in diffuse large B cell lymphoma by dynamic multidimensional single-cell profiling. *Nat Cancer*. 2024;5(7):1010-1023.

56. Haradhvala NJ, Leick MB, Maurer K, et al. Distinct cellular dynamics associated with response to CAR-T therapy for refractory B cell lymphoma. *Nat Med*. 2022;28(9): 1848-1859.

57. Talleur AC, Qudeimat A, Métais JY, et al. Preferential expansion of CD8+ CD19-CAR T cells postinfusion and the role of disease burden on outcome in pediatric B-ALL. *Blood Adv*. 2022;6(21):5737-5749.

58. Das RK, Vernau L, Grupp SA, Barrett DM. Naïve T-cell deficits at diagnosis and after chemotherapy impair cell therapy potential in pediatric cancers. *Cancer Discov*. 2019;9(4): 492-499.

59. Locke FL, Filosto S, Chou J, et al. Impact of tumor microenvironment on efficacy of anti-CD19 CAR T cell therapy or chemotherapy and transplant in large B cell lymphoma. *Nat Med*. 2024;30(2):507-518.